



HAL
open science

Resveratrol transformation in red wine after heat treatment

Toni El Khawand, Josep Valls Fonayet, Gregory da Costa, Ruth Hornedo-Ortega, Michael Jourdes, Céline Franc, Gilles de Revel, Alain Decendit, Stéphanie Krisa, Tristan Richard

► To cite this version:

Toni El Khawand, Josep Valls Fonayet, Gregory da Costa, Ruth Hornedo-Ortega, Michael Jourdes, et al.. Resveratrol transformation in red wine after heat treatment. Food Research International, 2020, 132, pp.1-6. 10.1016/j.foodres.2020.109068 . hal-03176116

HAL Id: hal-03176116

<https://hal.inrae.fr/hal-03176116>

Submitted on 22 Aug 2022

HAL is a multi-disciplinary open access archive for the deposit and dissemination of scientific research documents, whether they are published or not. The documents may come from teaching and research institutions in France or abroad, or from public or private research centers.

L'archive ouverte pluridisciplinaire **HAL**, est destinée au dépôt et à la diffusion de documents scientifiques de niveau recherche, publiés ou non, émanant des établissements d'enseignement et de recherche français ou étrangers, des laboratoires publics ou privés.



Distributed under a Creative Commons Attribution - NonCommercial| 4.0 International License

1 **Resveratrol transformation in red wine after heat treatment**

2

3 Toni El Khawand¹, Josep Valls Fonayet, Grégory Da Costa, Ruth Hornedo-Ortega,
4 Michael Jourdes, Céline Franc, Gilles de Revel, Alain Decendit, Stéphanie Krisa, Tristan
5 Richard*

6

7 *Unité de Recherche Œnologie, EA 4577, USC 1366 INRA, Bordeaux INP, Institut des*
8 *Sciences de la Vigne et du Vin, 210 Chemin de Leysotte, 33882 Villenave d'Ornon, France*

9

10

11

12

13

14

15

16

17

18

19 Corresponding author: Tristan Richard, email: tristan.richard@u-bordeaux.fr

20 ORCID Tristan Richard: 0000-0002-5308-8697

21

22 **Abstract**

23 Resveratrol is a well-known wine constituent. Its concentration can vary according to the
24 cultivar choice and the winemaking process. Due to its phenolic structure, resveratrol could
25 be transformed under high temperature or oxidative conditions, leading to the formation of
26 various derivatives including oligomers. Hence, the goal of this study is to investigate the
27 presence of these derivatives in wine. In the first stage, hemisynthesis of oligomeric stilbenes
28 was achieved from resveratrol in ethanol by oxidative coupling using metals. Four *de novo*
29 synthesized resveratrol derivatives were identified by MS and NMR spectroscopy including
30 two new molecules, oxistilbenin F and oxistilbenin G. In the second stage, analysis of red
31 wine after heat treatment by LC-MS confirmed the presence of some of these compounds in
32 wine. Finally, the anti-inflammatory effects of the compounds were evaluated by studying
33 their ability to prevent lipopolysaccharide (LPS)-induced upregulation of nitric oxide (NO)
34 and reactive oxygen species (ROS) production in RAW 264.7 macrophage cell line.

35

36 **Keywords**

37 resveratrol; stilbene; hemisynthesis; wine; oxidative coupling; anti-inflammatory effect

38

39 **1. Introduction**

40 Polyphenols are among the most valuable compounds found in wine and play a major role in
41 the taste and colour of wine and its potential biological activity (Garrido & Borges, 2013;
42 Quideau, Deffieux, Douat-Casassus, & Pouységu, 2011; Waterhouse, 2002). Most of these
43 compounds such as anthocyanins or tannins are subject to transformations in wines mainly
44 due to oxidative processes influencing the wine properties (Garrido & Borges, 2013). Among
45 them, stilbenes have received great attention. Originally identified in the grapevine and other
46 plants as phytoalexins, (Adrian, Jeandet, Veneau, A. Weston, & Bessis, 1997; Langcake &
47 Pryce, 1977), stilbenes were particularly studied for their several biological effects (Biais et
48 al., 2017; Vang et al., 2011; Zamora-Ros et al., 2008). Resveratrol and its glucoside, the
49 piceid, have the highest concentrations in wine among stilbenes (Guerrero, Valls-Fonayet,
50 Richard, & Cantos-Villar, 2020). Their initial concentrations in grape and wine depend on
51 several biotic and abiotic factors such as environmental stresses, the cultivar, and
52 technological practices (Fernández-Marín, Puertas, Guerrero, García-Parrilla, & Cantos-
53 Villar, 2014; Poussier, Guilloux-Benatier, Torres, Heras, & Adrian, 2003). Their final
54 concentrations in wine are the result of different mechanisms including enzymatic and
55 microbiological interactions, or oxidative reactions. It was demonstrated that piceid can be
56 hydrolysed during fermentation to produce resveratrol, by the yeast β -glucosidases (Roldán,
57 Palacios, Caro, & Pérez, 2010). Resveratrol *cis-trans* isomerization balance can also be
58 altered in wine under light exposure (Mattivi, Reniero, & Korhammer, 1995). In addition,
59 resveratrol can be oxidized in wine kept under heat and oxygen exposure due to its phenolic
60 structure (Bavaresco, Lucini, Busconi, Flamini, & de Rosso, 2016). In fact, oxidative
61 coupling of resveratrol could occur in presence of metallic catalysts like silver, iron or copper
62 in different solvents (Sako, Hosokawa, Ito, & Inuma, 2004; Velu et al., 2008). The conditions
63 required to induce these reactions can occur naturally in wine, through the presence of ethanol

64 and several metallic constituents, mainly iron and copper (Płotka-Wasyłka, Frankowski,
65 Simeonov, Polkowska, & Namieśnik, 2018; Tariba, 2011). In this study, the oxidative
66 coupling reaction protocol was adapted to obtain new resveratrol dimers in ethanol using
67 silver acetate (AgOAc) and iron chloride (FeCl₃), in the aim of investigate the presence of
68 these stilbenes in wine. Compounds were identified by mass spectrometry (MS) and nuclear
69 magnetic resonance (NMR) analysis. After identification of the *de novo* produced stilbenes,
70 their content was determined in red wine before and after heat treatment using a liquid
71 chromatography triple quadrupole tandem mass spectrometry (LC-QqQ-MS) method. Finally,
72 their ability to prevent lipopolysaccharide (LPS)-induced upregulation of nitric oxide (NO)
73 and reactive oxygen species (ROS) production in RAW 264.7 macrophage cell line were
74 investigated and compared to that of resveratrol.

75

76 **2. Material and methods**

77 **2.1. Analytical standards and reagents**

78 All reagents were of analytical grade and used as received without further purification.
79 Methanol (MeOH, HPLC grade), ethanol (HPLC grade), acetonitrile (HPLC and LC-MS
80 grades, purity $\geq 99.9\%$) and formic acid (98%) were purchased from Fisher scientific
81 (Loughborough, United Kingdom). Ethyl acetate (HPLC grade), ferric chloride (FeCl₃),
82 Dulbecco's Modified Eagle's Medium (DMEM) and Roswell Park Memorial Institute
83 (RPMI) culture media, foetal bovine serum (FBS), penicillin-streptomycin,
84 lipopolysaccharide (LPS), glutamine, methylthiazolyldiphenyl-tetrazolium bromide (MTT),
85 dimethyl sulfoxide (DMSO), Griess reagent, 2',7'-dichlorodihydrofluorescein diacetate
86 (H₂DCFDA) were purchased from Sigma-Aldrich (Saint-Louis, USA). *Trans*-resveratrol
87 (3,4',5-trihydroxystilbene, purity $\geq 99\%$) was supplied by Bulk Powders™ (Colchester,
88 United Kingdom). Silver acetate (AgOAc, purity $\geq 99\%$) was purchased from Acros organics

89 (Geel, Belgium). Ultrapure water was obtained from an Elga apparatus (High Wycombe,
90 United Kingdom).

91

92 **2.2. Oxidative coupling of resveratrol in ethanol**

93 Based on the protocol described by Sako et al. (Sako et al., 2004), regioselective oxidative
94 coupling reaction was first conducted on 600 mg of resveratrol (0.6 g, 12 mmol) using
95 AgOAc (670 mg, 18 mmol) or FeCl₃ (2.9 g, 18 mmol) in ethanol (100%, 60 mL) instead of
96 methanol. The reaction mixture was stirred at temperatures ranged between 20 and 50°C. The
97 reaction was then stopped by cooling at 4°C and centrifuged at 4000 rpm for 5 min. Then, the
98 ethanolic fraction was collected and the solvent was removed under reduced pressure using a
99 rotary evaporator. The lyophilization of the fractions obtained from both AgOAc and FeCl₃
100 reactions afforded a dark yellow powder and a light brown powder respectively. Produced
101 compounds from both reactions were isolated and identified using high performance liquid
102 chromatography (HPLC), ultra-high-performance liquid chromatography method with diode
103 array detection (UHPLC-DAD) and NMR.

104

105 **2.3. Isolation and identification of the reaction products**

106 The preparative HPLC was performed on a Gilson PLC 2050 apparatus (Middleton, WI,
107 USA) equipped with an UV-visible (UV-VIS) detector. Elution was conducted on an Agilent
108 Zorbax SB-C18 column (21.2 mm × 250 mm, 7 μm). The reaction extract powder was
109 solubilized at 50 mg/mL in MeOH-H₂O (50/50; v/v). Extract was then eluted with a flow rate
110 of 20 mL/min using non-acidified ultrapure water (solvent A) and acetonitrile (solvent B),
111 according the following gradient: 35% B (0-2 min), 35-45% B (2-25 min), 45-100% B (25-26
112 min) and 100% B (26-31 min). The detection was set at 280 and 306 nm and the fractions
113 were automatically collected. The solvent was removed under reduced pressure and fractions

114 were lyophilized. The elution of the reaction mix produced 3 different fractions, the third one
115 being an isomeric mixture. An additional elution step was then necessary to separate the 2
116 isomers. The third fraction was eluted with a flow rate of 20 mL/min using non-acidified
117 ultrapure water (solvent A) and methanol (solvent B), according the following gradient: 53%
118 B (0-2 min), 53-56% B (2-25 min), 56-100% B (25-26 min) and 100% B (26-31 min).
119 Compounds purity was measured using an UHPLC-DAD Agilent 1290 series apparatus
120 (Santa Clara, Canada) equipped with an auto sampler module, a binary pump, a degasser, a
121 column heater/selector and an diode array detector (DAD). The elution was performed on an
122 Agilent SB-C18 (2.1 mm x 100 mm, 1.8 μ m) column at a flow rate of 0.4 mL/min, with
123 acidified water (0.1% formic acid, solvent A) and acidified acetonitrile (0.1% formic acid,
124 solvent B) according to the following gradient: 10% B (0.0-1.7 min), 10-20% B (1.7-3.4 min),
125 20-30% B (3.4-5.1 min), 30% B (5.1-6.8 min), 30-35% B (6.8-8.5 min), 35-60% B (8.5-11.9
126 min), 60-100% B (11.9-15.3 min), 100% B (15.3-17.0 min), 100-10% B (17.0-17.3 min).
127 Samples were injected at a concentration of 100 μ g/mL after solubilization in H₂O/MeOH
128 mixture (1/1, v/v). Purity of the isolated compounds was estimated to be greater than 90%.
129 The purified compounds structure was determined by ¹H-¹³C-NMR, using a Bruker Avance
130 III 600 NMR spectrometer (Rheinstetten, Germany). Exact mass was determined by infusion
131 on a Thermo Fischer Scientific Q Exactive Plus Orbitrap (Waltham, Massachusetts, USA) in
132 negative mode with the following parameters: mode full scan; scan range: *m/z* 100-800;
133 resolution: 280k; automatic gain control (AGC) target: 2e⁵; max ion injection: 30 ms. Heated
134 Electrospray Ionization (HESI) source parameters: spray voltage: 2700V; sheath gas flow
135 rate: 8; capillary temperature: 320°C.

136

137 **2.3.1 Quadrangularin B (2)**

138 Brown amorphous powder. ¹H-NMR (600 MHz, methanol-*d*₄): δ 0.94 (3H, d, *J* = 7.0 Hz),
139 2.94 (1H, m), 3.17 (1H, m), 3.32 (1H, dd, *J* = 3.0, 8.6 Hz), 3.45 (1H, t, *J* = 3.0 Hz), 3.99 (1H,
140 d, *J* = 8.6 Hz), 4.27 (1H, d, *J* = 8.6 Hz), 5.65 (1H, brs), 6.15 (2H, d, *J* = 1.9 Hz), 6.17 (1H, t, *J*
141 = 1.9 Hz), 6.23 (1H, d, *J* = 2.0 Hz), 6.72 (2H, *J* = 8.5 Hz), 6.75 (2H, d, *J* = 8.5 Hz), 6.86 (2H,
142 *J* = 8.5 Hz), 7.00 (2H, d, *J* = 8.5 Hz); ¹³C-NMR (150 MHz, methanol-*d*₄): δ 14.3, 54.4, 58.3,
143 60.5, 62.9, 84.1, 100.0, 101.1, 104.7, 105.1, 114.3, 114.4, 122.3, 128.1, 129.1, 131.8, 137.2,
144 146.1, 150.6, 154.2, 155.4, 156.9, 157.7; HRMS (ESI): *m/z* calcd for C₃₀H₂₇O₇ [M – H][–] *m/z*
145 499.1757, found to be 499.1756.

146

147 **2.3.2 δ-viniferin (3)**

148 Colorless amorphous powder. ¹H-NMR (600 MHz, methanol-*d*₄): δ 4.45 (1H, d, *J* = 8.1 Hz),
149 5.45 (1H, d, *J* = 8.1 Hz), 6.19 (2H, d, *J* = 2.1 Hz), 6.24 (1H, t, *J* = 2.1 Hz), 6.27 (1H, t, *J* =
150 2.0 Hz), 6.53 (2H, d, *J* = 2.0 Hz), 6.85 (2H, d, *J* = 8.6 Hz), 6.87 (1H, d, *J* = 8.2 Hz), 6.89 (1H,
151 d, *J* = 16.3 Hz), 7.05 (1H, d, *J* = 16.3 Hz), 7.23 (2H, d, *J* = 8.3 Hz), 7.24 (1H, *J* = 1.8 Hz),
152 7.43 (1H, dd, *J* = 1.8, 8.2 Hz); ¹³C-NMR (150 MHz, methanol-*d*₄): δ 57.1, 93.2, 101.6, 101.9,
153 104.9, 106.6, 109.4, 115.3, 123.1, 126.6, 127.7, 127.9, 128.2 (2C), 131.0, 131.7, 139.8, 144.4,
154 157.7, 158.8, 159.0, 159.7; HRMS (ESI): *m/z* calcd for C₂₈H₂₁O₆ [M – H][–] 453.1338, found
155 to be 453.1343.

156

157 **2.3.3 Oxistilbenin F (4)**

158 Colourless amorphous powder. ¹H and ¹³C-NMR, see [Table 2](#); HRMS (ESI): *m/z* calcd for
159 C₃₀H₂₇O₇ [M – H][–] *m/z* 499.1757, found to be 499.1770.

160

161 **2.3.4 Oxistilbenin G (5)**

162 Colorless amorphous powder. ¹H and ¹³C-NMR, see [Table 2](#); HRMS (ESI): *m/z* calcd for
163 C₃₀H₂₇O₇ [M – H][–] *m/z* 499.1757, found to be 499.1739.

164

165 **2.4. Wine treatment and stilbene content**

166 **2.4.1 Wine treatment protocol**

167 A volume of 50 mL of red wine was heated at 30°C, for 24 hours. Ethanol was eliminated
168 under reduced pressure before proceeding to afford an aqueous wine solution. The samples
169 were then reloaded with pure water to recover a volume of 50 mL to start the solid-phase
170 extraction (SPE) of stilbenes. Hypersep C18 SPE cartridges 5 mg (Thermo Scientific,
171 Rockwood, USA) were previously conditioned with 25 mL of methanol and 25 mL of water.
172 The 50 mL sample was then loaded on the cartridge and a clean-up step with 50 mL of water
173 was conducted. Stilbenes were eluted with 50 mL of methanol and concentrated with a
174 rotatory evaporator to a final volume of 20 mL with 50% methanol.

175

176 **2.4.2 Stilbene quantification in wine**

177 Stilbenes were controlled and quantified using triple quadrupole-mass spectrometry (QqQ-
178 MS) detection on an Agilent 1260 LC system from Agilent Technologies (Santa Clara, CA,
179 USA). Chromatographic separation was carried out on an Agilent Poroshell C18 (150 mm x
180 2.1 mm x 2.7 μm) column at 35°C with a binary solvent system composed by acidified water
181 (0.1 % formic acid, solvent A) and acidified acetonitrile (0.1% formic acid, solvent B). The
182 elution was conducted at a flow rate of 0.3 mL/min according to the following gradient: 5-
183 18% B (0-5 min); 18-46% B (5-15 min); 46-95% B (22-25 min); 95% B (25-27 min); 95-5%
184 (27-30 min). The volume of injection for standards and wine samples was 5 μL. The
185 chromatographic system was coupled to an Agilent 6430 Triple Quadrupole mass
186 spectrometer which worked with the following parameters: Drying gas: 11 L/min, Source

187 Temperature: 350°C, Voltage: 3000V. The analysis was performed in optimized multiple
188 reaction monitoring (MRM) conditions obtained by the infusion of pure compounds. For the
189 calibration curve, a solution of 50% methanol containing 10 mg/L of resveratrol,
190 quadrangularin B, δ -viniferin, Oxistilbenin F and Oxistilbenin G was prepared in order to
191 obtain standard solutions by successive 1:2 dilutions.

192

193 **2.5. Biological assays**

194 **2.5.1. Cell culture**

195 Murine macrophage cell line RAW 264.7 was obtained from American Type Culture
196 Collection (ATCC, Rockville, MD, USA). Cells were maintained in DMEM medium
197 supplemented with 10% heat-inactivated foetal bovine serum, 1% streptomycin and 100
198 U/mL penicillin, at 37°C in a humidified, 5% CO₂, 95% air atmosphere.

199 Cells were seeded in 96-well plates (50,000 cells/well). After 24 hours, cells were incubated
200 with increasing concentrations of resveratrol and analogs (1- 20 μ M) for 24 hours in the
201 presence or absence of LPS (0.1 μ g/mL), in white RPMI medium containing 4 mM of
202 glutamine.

203

204 **2.5.2. Cytotoxicity determination**

205 Cell viability was evaluated by monitoring the cell mitochondrial activity, using the MTT
206 reduction assay. MTT solution (0.5 mg/mL) was added to each well and the cells were
207 incubated for additional 3 hours at 37 °C. Then, the supernatant was removed, formazan
208 crystals were dissolved in DMSO and the absorbance was measured at 595 nm in a
209 spectrophotometer microplate reader (FLUOstarOptima, BMG Labtech).

210

211 **2.5.3. NO measurement**

212 The nitric oxide (NO) production was determined by measuring the nitrite content in the
213 culture supernatant. Equal volumes of the Griess reagent and the cell culture supernatant were
214 mixed. After 15 min at room temperature, the absorbance was measured at 540 nm
215 (FLUOstarOptima, BMG Labtech). Sodium nitrite standard solution was used to calculate NO
216 concentration.

217

218 **2.5.4. Intracellular ROS measurement**

219 Generation of and reactive oxygen species (ROS) in cells was analysed using a fluorometric
220 probe, 2',7'-dichlorodihydrofluorescein diacetate (H₂DCFDA). After treatment, medium was
221 removed, cells were washed with phosphate-buffered saline (PBS) and incubated in the
222 presence of 5 μ M H₂DCFDA at 37°C for 30 min. Then, the fluorescence intensity was
223 quantified using a spectrofluorometer (FLUOstarOptima, BMG Labtech). The wavelengths of
224 excitation and emission used to detect the ROS were 485 nm and 520 nm, respectively.

225

226 **2.6. Statistical analysis**

227 Experiments were performed in quadruplicate and repeated at least three times. All values
228 were represented as mean \pm standard error of the mean (SEM). Data were analysed by one-
229 way analysis of variance followed by a Dunnett's post-test using GraphPad Prism Software
230 (Sa Diego, CA, USA). Significance was set at $p < 0.05$.

231

232 **3. Results and discussion**

233 **3.1. Treatment of resveratrol by metals**

234 Resveratrol was mixed with silver acetate (AgOAc) or iron chloride (FeCl₃) in ethanol
235 followed by chromatographic purification using preparative HPLC and structure identification
236 by HRMS and NMR spectroscopy. The reaction between resveratrol and metals in ethanol led

237 to the formation of four main compounds: quadrangularin B (**2**), δ -viniferin (**3**), oxistilbenin F
238 (**4**), and oxistilbenin G (**5**), as shown in [Table 1](#) and [Figure 1](#).

239 Compound **2** was identified as quadrangularin B (Adesanya et al., 1999). The relative
240 stereochemistry of quadrangularin B (**2**) was supported by the examination of ROESY
241 spectrum. The stereochemistry of C-7b and C-8b was established by the presence of NOE
242 correlations H-7b/H-10b and H-8b/H-2b. The correlations H-8a/H-10b and H-8a/H-7b
243 indicated that H-8a and H-7b are one the same side. Finally, NOE cross-peaks H-2a/H-14a
244 and H-2b/H-1 indicated the stereochemistry of C-1 (Adesanya et al., 1999). Compound **3** was
245 the main compound formed (yield 48% in AcOAg, after 1 h at 50°C). The structure of
246 compound **3** was identified as δ -viniferin by comparison with previously reported mass and
247 NMR data (Pezet et al., 2003). The $^1\text{H-NMR}$ spectrum of δ -viniferin (**3**) exhibited the
248 characteristic signals for the dihydrobenzofuran ring at δ 5.45 (d, $J = 8.1$ Hz) and 4.45 (d, $J =$
249 8.1 Hz), and for the *trans* vinyl protons at δ 7.05 (d, $J = 16.3$ Hz) and 6.89 (d, $J = 16.3$ Hz).
250 Compound **4** was obtained as an amorphous brown powder, with a high-resolution molecular
251 ion in negative mode at m/z $[\text{M} - \text{H}]^-$ 499.1770 (calcd for $\text{C}_{30}\text{H}_{27}\text{O}_7$ m/z 499.1757)
252 corresponding to a resveratrol dimer. The $^1\text{H-NMR}$ spectrum of compound **4** ([Table 2](#))
253 exhibited two AB_2 systems at δ 6.14 (1H, brs, H-12a), 6.41 (2H, d, $J = 2.1$ Hz, H-10a/14a),
254 and δ 6.14 (1H, brs, H-12b), 6.26 (2H, d, $J = 2.1$ Hz, H-10b/14b) for rings A_2 and B_2 ,
255 respectively; two $\text{AA}'\text{XX}'$ type ortho-coupled aromatic protons at δ 7.28 and 6.72 (2H each, d,
256 $J = 8.6$ Hz) for ring A_1 , δ 6.72 and 7.12 (2H each, d, $J = 8.7$ Hz) for ring B_1 ; two *trans*
257 coupled olefinic bond proton signals at δ 6.77 (1H, d, $J = 16.1$ Hz, H-8a) and 6.90 (1H, d, $J =$
258 16.1Hz, H-7a), two coupled aliphatic protons at δ 4.44 (1H, d, $J = 5.8$ Hz, H-7b) and 5.10
259 (1H, d, $J = 5.8$ Hz, H-8b), and one ethoxy group at δ 1.08 (3H, $J = 7.0$ Hz), 3.28 (1H, m) and
260 3.42 (1H, m). The correlations of the aromatic rings, double bond, aliphatic protons were
261 deduced from COSY spectrum. All the protonated carbons were identified from HSQC

262 spectrum. The examination of the C-H long range correlations from HMBC spectrum
263 indicated that compound **4** was a chain resveratrol dimer connected with C-8b and OH-4a.
264 This connectivity was confirmed by the HMBC cross-peaks C-3a/H-8b and C-8b/H10b. The
265 position of the ethoxy group was deduced from the HMBC cross-peak between OCH₂ and H-
266 7b. Concerning relative stereochemistry, the absence of strong NOE correlations H-8b/H-2b
267 and H-7b/H10b indicated that C-7b and C-8b should be in *threo* form. The structure of the
268 new compound **4** was named oxistilbenin F. Compound **5** was obtained as a brown
269 amorphous powder, with a high-resolution molecular ion in negative mode at m/z [M – H]⁻
270 499.1739 (calcd for C₃₀H₂₇O₇ m/z , 499.1757). The NMR data (Table 2) of **5** were nearly
271 identical to those of oxistilbenin F (**4**). Examination of 2D NMR spectra suggested that
272 compounds **4** and **5** are a pair diastereoisomers. In contrast to ROESY spectrum of
273 oxistilbenin F (**4**), the strong NOE cross-peaks H-8b/H-2b and H-7b/H10b observed for
274 compound **5** suggested that C-7b and C-8b should be in *erythro* form. In addition, the large
275 and small values for H-7b and H-8b measured for *erythro* and *threo* forms, respectively,
276 were in agreement with thus observed in close diastereoisomers (Li et al., 2017). The
277 structure of the new compound **5** was named oxistilbenin G.

278 As previously observed, metals induce resveratrol dimerization by oxidative coupling (Sako
279 et al., 2004; Velu et al., 2008). The reaction can be explained by a single electron transfer
280 from resveratrol to metal cation followed by a regioselective coupling and intramolecular
281 cyclization. The dimerization process is mainly controlled by the one-electron oxidant and the
282 solvent used (Sako et al., 2004; Velu et al., 2008). The efficiency of the reaction (Table 1)
283 depends of the oxidation ability of the employed oxidative reagents and temperature. In all
284 cases, δ -viniferin (**3**) was the major product and quadrangularin B (**2**) and oxistilbenin F (**4**)
285 were obtained as minor products. Comparing the metallic catalysts used, the reaction is much
286 more effective with silver acetate (total yield 87%, after 1 hour at 50°C) than with FeCl₃ (total

287 yield 18%, after 1 hour at 50°C). When FeCl₃ was employed, quadrangularin B (**2**) and
288 oxistilbenin F (**4**) were hardly produced, while δ-viniferin (**3**) and oxistilbenin G (**5**) were
289 formed in lower quantities. The mechanism of formation of the different dimers could be
290 similar to that reported for isorhapontigenin (Wang et al., 2014). In fact, the oxidative reaction
291 on OH-4 position could induce the formation of phenoxy radicals leading large diversity of
292 coupling modes. Quadrangularin B (**2**) was previously obtained by biomimic transformation
293 of resveratrol using peroxidases (Takaya et al., 2005). Oxistilbenin F (**4**) and G (**5**) were
294 synthesized and reported for the first time.

295

296 **3.2. Formation of resveratrol dimers in wine after heat treatment**

297 Resveratrol is one of the main stilbenes identified in wines. Even if its amount vary greatly,
298 its average content is 2.7 mg/L in red wines (Neveu et al., 2010). In addition, oxidative
299 reagents, such iron, are naturally present in wine (Tariba, 2011). Based on the results obtained
300 in this work, resveratrol dimerization could occur in wine. To confirm this hypothesis, a red
301 wine was subjected to a heat treatment at 30°C for 24 hours. Stilbenes were quantified before
302 and after wine heating using a LC-MS method on a triple quadrupole mass spectrometer (LC-
303 QqQ-MS). MRM mode was used to select specific transitions of the quantified compounds in
304 order to increase both selectivity and sensitivity (Lambert et al., 2015). For each compound,
305 MRM transitions parameters were optimised. The optimised MRM transition parameters are
306 shown in [Table 3](#). For quantitative analysis, the quantifier transition chromatogram of stilbene
307 was used, and the rest of transitions confirmed the stilbene identification in wine. The
308 quantifier transitions were *m/z* 227/143 for resveratrol (**1**), *m/z* 499/359 for
309 quadrangularin B (**2**), *m/z* 453/361 for δ-viniferin (**3**), *m/z* 499/227 for oxistilbenin F (**4**), and
310 *m/z* 499/453 for oxistilbenin G (**5**).

311 The amounts of the five quantified stilbenes before and after wine treatment were reported in
312 [Table 4](#). Before wine treatment, the level of resveratrol was found to be 330 µg/L in the red
313 wine. In addition, a small amount of δ-viniferin was observed (20 µg/L). This compound is a
314 natural stilbene previously identified in red wine (Vitrac et al., 2005). After wine treatment
315 for 24 hours at 30°C, the level of resveratrol had decreased by almost 50%, while the amount
316 of δ-viniferin had increased by 5-fold bringing it from 20 to 100 µg/L. In addition, the
317 formation of oxistilbenin G was observed in red wine after the heat treatment. This compound
318 was specifically formed after oxidative coupling of two resveratrol units in ethanol. The
319 δ-viniferin was the main compound formed in red wine followed by oxistilbenin G, in
320 agreement with the rate observed in the reaction between resveratrol and metals in ethanol
321 ([Table 1](#)). All these data have confirmed that resveratrol could be transformed by oxidative
322 coupling during wine aging providing oligomers. The difference between the total stilbene
323 content before and after treatment (1.50 and 0.94 µM, respectively) seems to indicate that a
324 part of the resveratrol reacted with other compounds.

325

326 **3.3. Anti-inflammatory activity of resveratrol derivatives**

327 Anti-inflammatory activity of the produced compounds was evaluated using LPS-induce
328 RAW 264.7 cells model. In order to determine the cytotoxicity of stilbenes, the viability was
329 measured after cells treatment at 1 to 20 µM. Resveratrol and quadrangularine B did not show
330 significant cytotoxicity at all tested concentrations, whereas δ-viniferin, oxistilbenin F and
331 oxistilbenin G exhibited cellular toxicity at 15 µM (data not shown). On one hand, as shown
332 in the [Fig. 2A](#), resveratrol, δ-viniferin, oxistilbenin F and oxistilbenin G reduced NO
333 production by LPS-stimulated macrophages, with IC₅₀ of 17.9, 8.7, 9.2 and 9.8 µM,
334 respectively. On the other hand, quadrangularin B exhibited a moderate inhibitory activity
335 against NO at the highest concentration. In addition, a decrease effect on the production of

336 ROS was observed for all stilbenes except the quadrangularin B (Fig. 2B). The δ -viniferin
337 was the most effective (IC₅₀ 7.6 μ M). Thus, oxidative coupling during wine aging could
338 modulate the biological activities associated with red wine stilbenes. This study confirms that
339 red wine storage temperature is an important consideration to preserve wine properties.

340

341 **4. Conclusion**

342 In this study, we demonstrated that oxidative dimerization of resveratrol could occur in red
343 wine after heat treatment. Heating the wine modulates the stilbene content by reducing the
344 resveratrol amount, increasing the amount of δ -viniferin, and inducing the formation of new
345 compounds such as oxistilbenin G. Finally, the anti-inflammatory activity of these
346 compounds was evaluated. The results have indicated that oxidative coupling during wine
347 aging could modulate the biological properties of wine by inducing the formation of more
348 active compounds such δ -viniferin.

349

350 **Acknowledgements**

351 The work was supported by the Bordeaux Metabolome Facility and MetaboHUB (ANR-11-
352 INBS-0010 project).

353

354 **References**

- 355 Adesanya, S. A., Nia, R., Martin, M. T., Boukamcha, N., Montagnac, A., & Païs, M. (1999).
356 Stilbene derivatives from *Cissus quadrangularis*. *Journal of Natural Products*, 62 (12),
357 1694-1695.
- 358 Adrian, M., Jeandet, P., Veneau, J., A. Weston, L., & Bessis, R. (1997). Biological activity of
359 resveratrol, a stilbenic compound from grapevines, against *Botrytis cinerea*, the causal
360 agent for gray mold. *Journal of Chemical Ecology*, 23, 1689-1702.
- 361 Bavaresco, L., Lucini, L., Busconi, M., Flamini, R., & de Rosso, M. (2016). Wine resveratrol:
362 From the ground up. *Nutrients*, 8 (4).
- 363 Biais, B., Krisa, S., Cluzet, S., Da Costa, G., Waffo-Teguo, P., Mérillon, J. M., & Richard, T.
364 (2017). Antioxidant and cytoprotective activities of grapevine stilbenes. *Journal of*
365 *Agricultural and Food Chemistry*, 65 (24), 4952-4960.

366 Fernández-Marín, M. I., Puertas, B., Guerrero, R. F., García-Parrilla, M. C., & Cantos-Villar,
367 E. (2014). Preharvest Methyl Jasmonate and Postharvest UVC Treatments: Increasing
368 Stilbenes in Wine. *Journal of Food Science*, 79 (3), C310-C317.

369 Garrido, J., & Borges, F. (2013). Wine and grape polyphenols — A chemical perspective.
370 *Food Research International*, 54 (2), 1844-1858.

371 Guerrero, R. F., Valls-Fonayet, J., Richard, T., & Cantos-Villar, E. (2020). A rapid
372 quantification of stilbene content in wine by ultra-high pressure liquid
373 chromatography – Mass spectrometry. *Food Control*, 108.

374 Lambert, M., Meudec, E., Verbaere, A., Mazerolles, G., Wirth, J., Masson, G., Cheynier, V.,
375 & Sommerer, N. (2015). A High-Throughput UHPLC-QqQ-MS Method for
376 Polyphenol Profiling in Rosé Wines. *Molecules*, 20 (5), 7890-7914.

377 Langcake, P., & Pryce, R. J. (1977). A new class of phytoalexins from grapevines.
378 *Experientia*, 33 (2), 151-152.

379 Li, W., Dong, T., Chen, P., Liu, X., Liu, M., & Han, X. (2017). Concise synthesis of several
380 oligostilbenes from the enzyme-promoted oxidation of brominated resveratrol.
381 *Tetrahedron*, 73 (21), 3056-3065.

382 Mattivi, F., Reniero, F., & Korhammer, S. (1995). Isolation, Characterization, and Evolution
383 in Red Wine Vinification of Resveratrol Monomers. *Journal of Agricultural and Food
384 Chemistry*, 43 (7), 1820-1823.

385 Neveu, V., Perez-Jiménez, J., Vos, F., Crespy, V., du Chaffaut, L., Mennen, L., Knox, C.,
386 Eisner, R., Cruz, J., Wishart, D., & Scalbert, A. (2010). Phenol-Explorer: an online
387 comprehensive database on polyphenol contents in foods. *Database*, 2010, bap024.

388 Pezet, R., Perret, C., Jean-Denis, J. B., Tabacchi, R., Gindro, K., & Viret, O. (2003). δ -
389 viniferin, a resveratrol dehydrodimer: one of the major stilbenes synthesized by
390 stressed grapevine leaves. *Journal of Agricultural and Food Chemistry*, 51 (18), 5488-
391 5492.

392 Płotka-Wasyłka, J., Frankowski, M., Simeonov, V., Polkowska, Ż., & Namieśnik, J. (2018).
393 Determination of Metals Content in Wine Samples by Inductively Coupled Plasma-
394 Mass Spectrometry. *Molecules (Basel, Switzerland)*, 23 (11), 2886.

395 Poussier, M., Guilloux-Benatier, M., Torres, M., Heras, E., & Adrian, M. (2003). Influence of
396 Different Maceration Techniques and Microbial Enzymatic Activities on Wine
397 Stilbene Content. *American Journal of Enology and Viticulture*, 54 (4), 261-266.

398 Quideau, S., Deffieux, D., Douat-Casassus, C., & Pouységu, L. (2011). Plant Polyphenols:
399 Chemical Properties, Biological Activities, and Synthesis. *Angewandte Chemie
400 International Edition*, 50 (3), 586-621.

401 Roldán, A., Palacios, V., Caro, I., & Pérez, L. (2010). Evolution of Resveratrol and Piceid
402 Contents during the Industrial Winemaking Process of Sherry Wine. *Journal of
403 Agricultural and Food Chemistry*, 58 (7), 4268-4273.

404 Sako, M., Hosokawa, H., Ito, T., & Iinuma, M. (2004). Regioselective oxidative coupling of
405 4-hydroxystilbenes: synthesis of resveratrol and ϵ -viniferin (E)-dehydrodimers.
406 *Journal of Organic Chemistry*, 69 (7), 2598-2600.

407 Takaya, Y., Terashima, K., Ito, J., He, Y.-H., Tateoka, M., Yamaguchi, N., & Niwa, M.
408 (2005). Biomimic transformation of resveratrol. *Tetrahedron*, 61 (43), 10285-10290.

409 Tariba, B. (2011). Metals in wine - Impact on wine quality and health outcomes. *Biological
410 Trace Element Research*, 144 (1-3), 143-156.

411 Vang, O., Ahmad, N., Baile, C. A., Baur, J. A., Brown, K., Csiszar, A., Das, D. K., Delmas,
412 D., Gottfried, C., Lin, H. Y., Ma, Q. Y., Mukhopadhyay, P., Nalini, N., Pezzuto, J. M.,
413 Richard, T., Shukla, Y., Surh, Y. J., Szekeres, T., Szkudelski, T., Walle, T., & Wu, J.
414 M. (2011). What is new for an old molecule? systematic review and recommendations
415 on the use of resveratrol. *PloS One*, 6 (6).

- 416 Velu, S. S., Buniyamin, I., Ching, L. K., Feroz, F., Noorbacha, I., Gee, L. C., Awang, K.,
417 Wahab, I. A., & Weber, J.-F. F. (2008). Regio- and stereoselective biomimetic
418 synthesis of oligostilbenoid dimers from resveratrol analogues: influence of the
419 solvent, oxidant, and substitution. *Chemistry--A European Journal*, 14 (36), 11376-
420 11384.
- 421 Vitrac, X., Bornet, A., Vanderlinde, R., Valls, J., Richard, T., Delaunay, J. C., Mérillon, J. M.,
422 & Teissédre, P. L. (2005). Determination of stilbenes (δ -viniferin, trans-astringin,
423 trans-piceid, cis- and trans-resveratrol, ϵ -viniferin) in Brazilian wines. *Journal of*
424 *Agricultural and Food Chemistry*, 53 (14), 5664-5669.
- 425 Wang, X.-F., Zhang, Y., Lin, M.-B., Hou, Q., Yao, C.-S., & Shi, J.-G. (2014). Biomimetic
426 synthesis of active isorhapontigenin dimers. *Journal of Asian Natural Products*
427 *Research*, 16 (5), 511-521.
- 428 Waterhouse, A. L. (2002). Wine Phenolics. *Annals of the New York Academy of Sciences*, 957
429 (1), 21-36.
- 430 Zamora-Ros, R., Andres-Lacueva, C., Lamuela-Raventós, R. M., Berenguer, T., Jakszyn, P.,
431 Martínez, C., Sánchez, M. J., Navarro, C., Chirlaque, M. D., Tormo, M. J., Quirós, J.
432 R., Amiano, P., Dorronsoro, M., Larrañaga, N., Barricarte, A., Ardanaz, E., &
433 González, C. A. (2008). Concentrations of resveratrol and derivatives in foods and
434 estimation of dietary intake in a Spanish population: European Prospective
435 Investigation into Cancer and Nutrition (EPIC)-Spain cohort. *British Journal of*
436 *Nutrition*, 100 (1), 188-196.
- 437
- 438

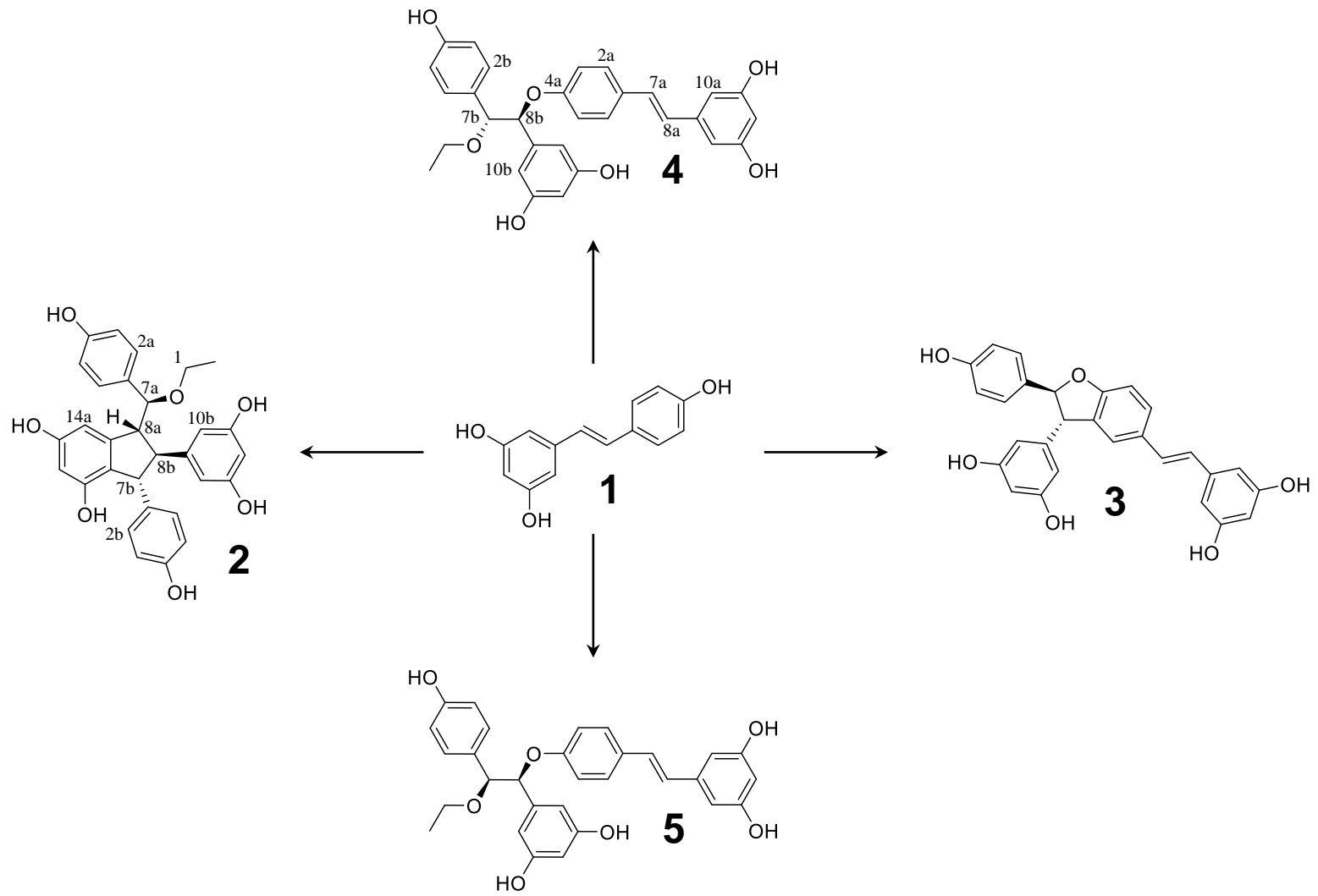
439 **Figure legends**

440 **Figure 1.** Structures of the compounds formed after oxidative coupling of resveratrol.

441

442 **Figure 2.** Effect of treatment with stilbene and LPS (0.1 $\mu\text{g}/\text{mL}$) on the NO production (A) or
443 ROS formation (B) in RAW 264.7 cells. Res = resveratrol, δ -vin = δ -viniferin, Oxi F =
444 oxistilbenin F, Oxi G = oxistilbenin G and Qua B = quadrangularin B. Data are expressed as
445 percentage of the control (cells treated with LPS alone set to 100% production),
446 corresponding to the mean \pm SEM (n=4).

447



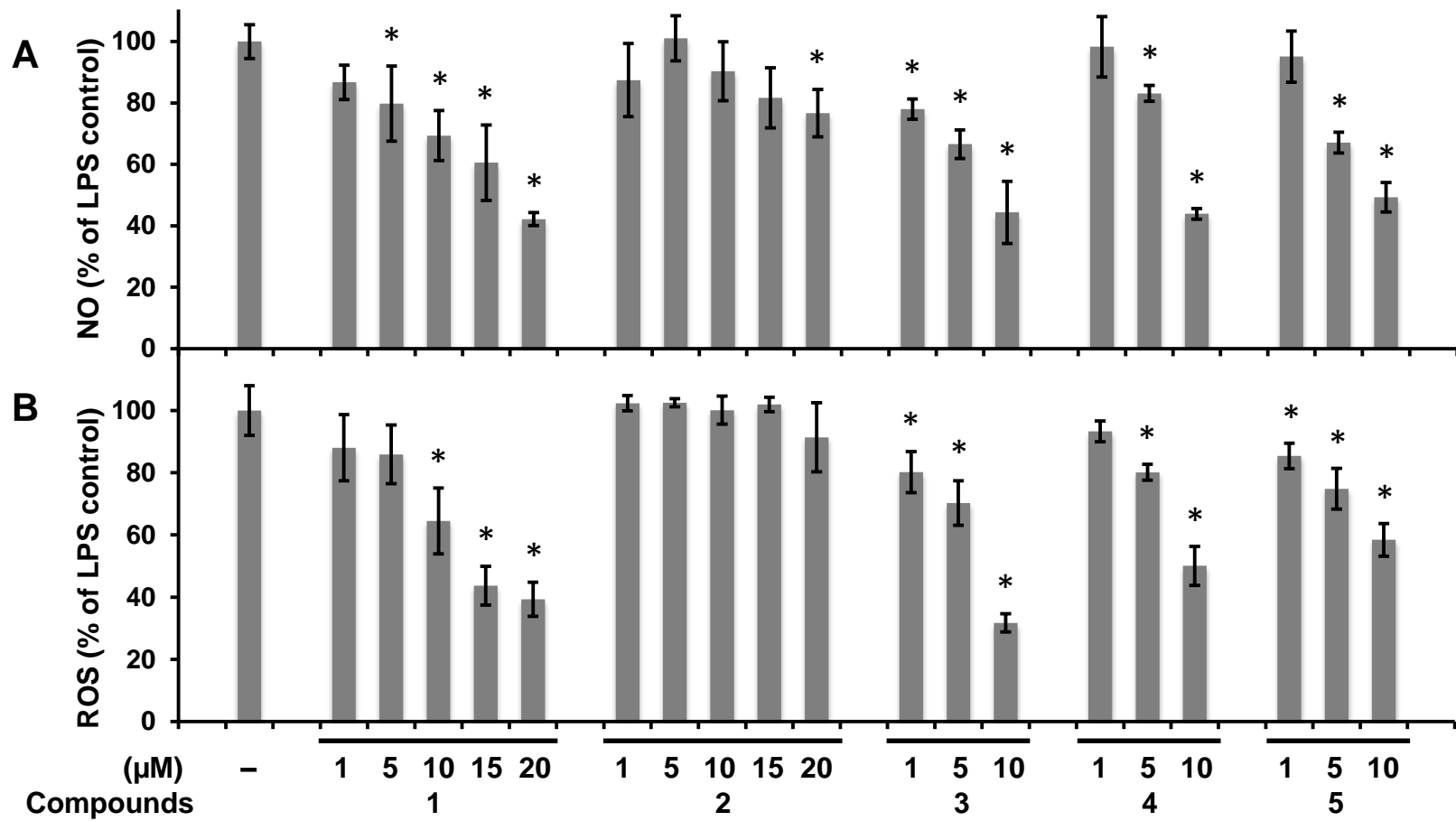


Table 1. Treatments of resveratrol (**1**) with different oxidizing reagents in ethanol.

Reagent	Temperature (°C)	Time (h)	Yield (%)			
			2	3	4	5
AgOAc	50	1	3	48	6	32
AgOAc	40	1	2	29	4	19
AgOAc	40	2	2	33	5	22
AgOAc	30	1	0	15	2	10
AgOAc	20	1	0	3	0	0
FeCl ₃	50	1	1	10	1	6

Table 2. NMR data of compounds **4** and **5** in methanol-*d*₄.

	4		5	
	δ_C	δ_H (mult., <i>J</i> in Hz)	δ_C	δ_H (mult., <i>J</i> in Hz)
1a	130.2	-	130.2	-
2a/6a	127.1	7.28 (d, 8.7)	127.1	7.33 (d, 8.7)
3a/5a	115.1	6.72 (d, 8.7)	115.2	6.85 (d, 8.7)
4a	157.9	-	158.1	-
7a	127.8	6.90 (d, 16.1)	127.8	6.92 (d, 16.1)
8a	126.6	4.24 (d, 16.1)	126.6	6.79 (d, 16.1)
9a	139.7	-	139.7	-
10a/14a	104.6	6.41 (d, 2.1)	104.6	6.42 (d, 2.1)
11a/13a	158.2	-	158.3	-
12a	101.4	6.14 (brs)	101.4	6.14 (t, 2.1)
1b	129.2	-	128.8	-
2b/6b	129.2	7.12 (d, 8.7)	128.8	6.99 (d, 8.7)
3b/5b	114.3	6.72 (d, 8.7)	114.2	6.66 (d, 8.7)
4b	156.7	-	156.7	-
7b	84.7	4.44 (d, 5.8)	85.2	4.52 (d, 6.9)
8b	82.7	5.10 (d, 5.8)	83.9	5.05 (d, 6.9)
9b	141.4	-	140.6	-
10b/14b	105.8	6.26 (d, 2.1)	106.0	6.11 (d, 2.1)
11b/13b	157.8	-	157.8	-
12b	101.4	6.14 (brs)	101.4	6.05 (t, 2.1)
OCH ₂	64.6	3.28 (m) 3.42 (m)	64.6	3.46 (m)
CH ₃	14.1	1.08 (t, 7.0)	14.1	1.17 (t, 7.0)

Table 3. MRM parameters (precursor and product ions m/z , retention times), and quantitative response of stilbene compounds in wine.

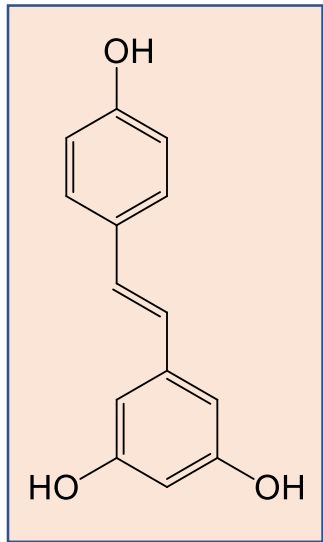
Compound	Formula	Mode	Precursor ion m/z	Quantifier m/z	Qualifiers m/z	Retention time (min.)	Calibration range (mg/L)
resveratrol (1)	C ₁₄ H ₁₂ O ₃	-	227	143	185	19.86	0.039-2
quadrangularin B (2)	C ₃₀ H ₂₈ O ₇	-	499	359	255, 289	19.57	0.0048-1.25
δ -viniferin (3)	C ₂₈ H ₂₂ O ₆	-	453	361	227, 107, 215	21.57	0.0097-1.25
oxistilbenin F (4)	C ₃₀ H ₂₈ O ₇	-	499	227	271, 453, 225	22.14	0.0048-1.25
oxistilbenin G (5)	C ₃₀ H ₂₈ O ₇	-	499	453	227, 271, 225	22.41	0.0048-1.25

Table 4. Stilbene levels in wine before and after heat treatment (24h at 30°C). Results are expressed in µg/L as means of 3 instrumental replicates ± SD.

Compound	Before heating	After heating
resveratrol (1)	330 ± 100	160 ± 100
quadrangularin B (2)	nd	nd
δ-viniferin (3)	20 ± 10	100 ± 10
oxistilbenin F (4)	nd	nd
oxistilbenin G (5)	nd	6 ± 1
Total	350 ± 110	266 ± 111

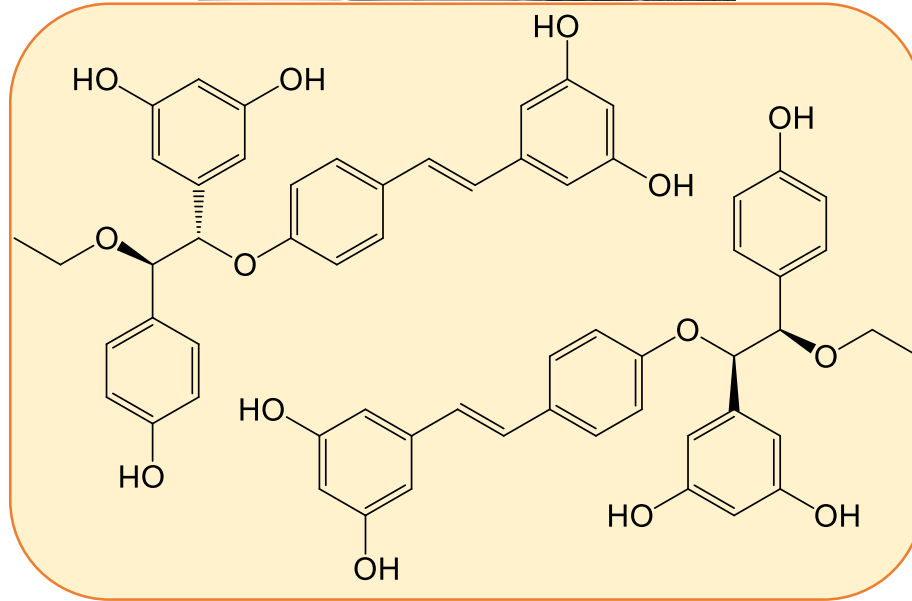


Investigation of their presence in red wine



Resveratrol oxidative coupling

Metals
Ethanol



Identification of new resveratrol dimers



Study of their anti-inflammatory activity *in vitro*